STUDY ON CRACKING OF RC BRIDGE PIERS RELATED WITH THE FAILURE MECHANISMS CAUSED BY THE EFFECTS OF THE 1995 GREAT HANSHIN EARTHQUAKE

Kobe University　Shiro Takada *
Kobe University　Hidenori Morikawa **
Kobe University　Freddy Duran C. ***

Summary

This study aims to analyze the cracking phenomena on the seismic response of reinforced concrete piers by using a nonlinear finite element approach based on an orthotropic fixed-smeared model in which the material nonlinearities are considered. The strain-softening is considered herein in order to take into account the progressive structural deterioration (associated with bond), and development of cracking failure. An attempt is also made to consider the bond performance of reinforcing steel bars embedded in the concrete by using bond-stress relationships. The analytical approach presented herein is then considered in the evaluation of the structural response of a RC single-column bent which meet similar characteristics with respect to those piers of the same type that sustained severe damage caused by the 1995 Great Hanshin Earthquake. At the end, the analytical results are evaluated which leads to conclusions and recommendations which in turn may be taken into account in the understanding of the cracking phenomena in the seismic response of RC bridge piers.

1. Introduction

The seismic damage to bridge structures caused by the 1995 Great Hanshin Earthquake was strongly influenced by the failure mechanism to supporting reinforced concrete piers. Damage assessment based on surveys on the overall highways and railways in the quake-hit[1] area make to be possible to infer that, the nature of the progressive structural deterioration associated with bond, and the development of cracking failure represent the most important tasks to analyze in order to understand in deep the failure mechanism and damage to RC piers that lead to their collapse during an strong earthquake.

The aforementioned implies that crack modeling of RC structures under cyclic reversals represents one of the most important problems to solve, especially, when finite element techniques are used. Consequently, this study is advocated in the understanding of cracking phenomena on failure mechanisms of RC bridge piers during a strong shaking. Particular emphasis is given to the RC single-column bents with similar characteristics to those piers collapsed by the 1995 Great Hanshin Earthquake.

2. Outline of earthquake damage to bridges

The 1995 Great Hanshin Earthquake with magnitude 7 on the japanese scale (7 is the maximum magnitude according to the Japanese Meteorological Agency) or M=7.2 on the Richter scale, hit southern Hyogo Prefecture. Maximum quake-intensities affected also the northern Awajishima Island. The levels of acceleration in both horizontal (400 gals) and vertical direction (200 gals) considered usually in the seismic design of railway tracks and buildings, were widely exceeded in many places. Elevated viaducts on highways wrecked especially along the Hanshin Expressway (Kobe Route 3, Wangan Route 5, and Kita-Kobe Route), the Meishin Expressway, the Chugoku Expressway, the Route 2, and also on railways including the bullet train line's elevated tracks. Most of these structures were designed in the late 1960s and early 1970s. Particularly dramatic was the case of a single row of 17 huge T-shape RC single-column bents (*Piltz type*) spaced at about 35 meters with the next holding up concrete girders in a 635-m section of the Hanshin Expressway which did not withstand the strong shaking of about 600-800 gals, then snapped and caused the section to be tumbled sideways, exposing the steel reinforcement and the deficient design of the piers. The section was built in the late 1960s, following the *piltz method* of construction in which the vertical and horizontal parts of the piers are constructed as a single concrete unit in the form of a *mushroom* , without joints (See Fig. 1).

An on-site inspection on the fell section as well as in other sections along the Hanshin Expressway indicates that:

- Butt weld of longitudinal reinforcement aligned at the same level around the perimeter in the lower part of the pier near the mid-height.
- Each RC pier damaged or fell off, was reinforced with approximately 200 steel reinforcing bars of about 35mm diameter. The shear reinforcement (hoops) was almost typical regardless the cross-section shape (rectangular or circular) or the size (Short or tall columns), hoops were 16mm diameter spaced typically at 30 cm centers.
- Piers were lack of enough detailing to provide sufficient ductility to withstand large deformations and rotations.

On the same way, failed columns supporting the elevated tracks of the shinkansen viaduct had longitudinal reinforcement given by approximately 29mm bars spaced at about 8 cm around the perimeter. The typical shear reinforcement was given by plain 9 mm diameter bars spaced about 30 cm centers.

In general terms, it is possible to state that the causes of failure or collapse of most of RC bridge piers during the 1995 Great Hanshin Earthquake were given by both the weakness of plastic hinge zones (critical zones) due to poor lateral reinforcement with deficient welding detailing, as well as, the deficient anchorage of transverse reinforcement, and, the insufficient end anchorage of reinforcing bars extending upward from the footing like dowells.

These structural deficiencies led to the lack of capacity to withstand both large deformations and large lateral forces.

Keywords : Bridge piers, reinforced concrete, cracking, failure mechanism, structural response

*　Kobe University, 078-803-1031
**　Kobe University, 078-803-1040
***　Kobe University, 078-881-1212　Ext. 2783

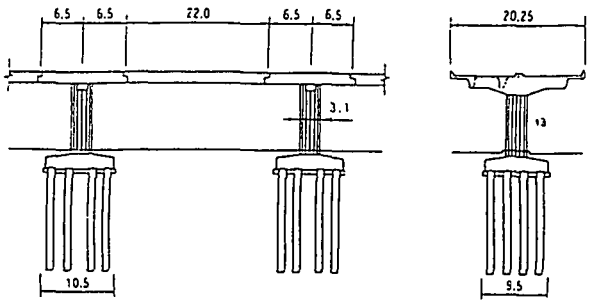

Fig. 1 Geometrical characteristics of a typical RC single-column bent of the Hanshin Expressway viaduct that collapsed by the effects of the 1995 Great Hanshin Earthquake

3. Constitutive modeling

The concrete material model is considered herein to be hypo-elastic, based on a uniaxial stress-strain relation. The model employs two basic features to describe the material behavior: 1) A nonlinear stress-strain relation for tension, including strain softening to allow for weakening of the material under tensile strength; 2) A failure envelope that defines cracking and crushing in compression as well as the post-cracking of the material by means of the progressive degradation of concrete. The steel reinforcement is represented as a uniaxial elasto-perfectly plastic work-hardening material in both tension and compression .

(1) Nonlinear stress-strain relationship for concrete in tension

The bi-linear softening model given by Eq. 1 and shown in Fig. 2 is used to represent the initial cracking and post-cracking stage of concrete in tension.

$$f'_t = 0.62 \, (f'_c)^{1/2} \quad \text{(MPa)} \qquad (1)$$
$$\varepsilon_{ot} = f'_t / E$$
$$\varepsilon_{ut} = 9.2 \, \varepsilon_{ot}$$

where,

f'_t = Tensile strength of unconfined concrete
ε_{ot} = Tensile cracking strain of concrete (initial tensile strain threshold)
ε_{ut} = Ultimate tensile strain of concrete. (In uniaxial and biaxial tension the average value of the maximum principal tensile strain is about 0.008).

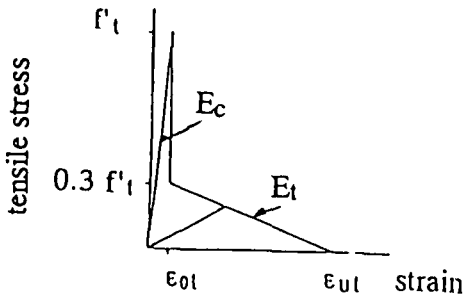

Fig. 2 Stress-strain relationship of concrete in tension considering softening in the post-cracking stage

(2) Nonlinear stress-strain relationship for concrete in compression

The failure envelope for concrete under uniaxial compression considered herein is shown in Fig. 3. The expressions for both the ascending and descending parts of this failure envelope are described by Eqs. 2 and 3 respectively which were originally obtained by Kim and Lee[2] - 1993 by fitting a large volume of test data from a number of researchers[3]. The lateral confinement and eccentric loading are improved herein by taking into account parameters related with the eccentricity of loads formulated in the stress-strain relationship for confined concrete proposed by Saatcioglu and Razvi[4] -1992.

a) Ascending part

The ascending part of the envelope of the stress-strain relationship for concrete under compression (See Fig. 3) is given by the following equation:

$$f_{cc} = f'_{cc} \left[A \, (\varepsilon_{cc} / \varepsilon_{occ}) - (A - 1) \, (\varepsilon_{cc} / \varepsilon_{occ})^{A/(A-1)} \right] \qquad (2)$$

where,

$A = E_c \varepsilon_{occ} / f_{occ}$
f_{cc} = Stress of confined concrete (MPa)
ε_{cc} = Compressive strain of confined concrete for uniaxial and biaxial compression.
f'_{cc} = Ultimate compressive strength of confined concrete (MPa)
f_{occ} = Peak stress of confined concrete (MPa)
ε_{occ} = Strain corresponding to peak stress of confined concrete (initial compressive strain threshold)
E_c = Elastic modulus of concrete (MPa)
f'_c = Concrete cylinder compressive strength (MPa)

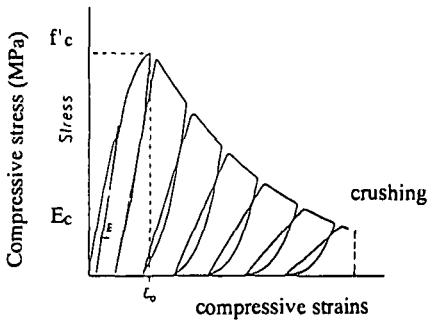

Fig. 3. Uniaxial stress-strain relationship for compression of concrete[2]

When stresses reach values near the compressive strength, at says, 75 percent of f'_c, the rate of crack propagation is assumed to increase although the rate of loading is kept constant. It leads to largest cracks to reach critical crack lengths. The complete rupture and desintegration of the concrete under compression stress is defined as crushing in which the concrete is assumed to lose its resistance completely against any deformation.

b) Descending part

The progressive degradation of concrete that causes significant changes in the material-stiffness matrix is defined by the envelope of unloading-reloading of the descending part of the curve described by Eq. 3 and depicted by Fig. 3

very difficult task especially if the analysis involves multiple reversals with cracks forming ramdonly as well as when material and/or geometrical nonlinearities are taken into account.

As can be seen, the major drawback with the use of quarter-point elements is the requirement of post-processing the stress-intensity factors from the FEM solutions.

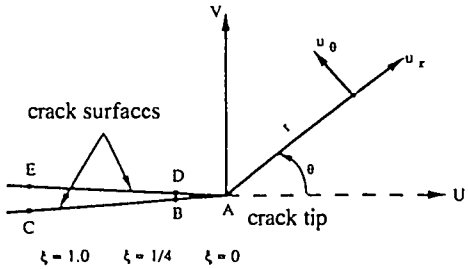

Fig. 5. Crack tip discretization and quarter-point positions

(2) Stress intensity factors for the opening and sliding cracking mechanism

For the combined opening and sliding cracking mechanism (i.e. types I and II, respectively), the stress intensity factors are determined from the relative displacements at element quarter points B and D (shown in Fig. 5) using the followinf equations.

$$K_I = [\,2\,G\,/\,(k+1)]\,\sqrt{(\pi\,/\,2r)}\,(V_D - V_B) \quad \text{kPa-m}^{1/2}$$
$$K_{II} = [\,2\,G\,/\,(k+1)]\,\sqrt{(\pi\,/\,2r)}\,(U_D - U_B) \quad \text{kPa-m}^{1/2} \qquad (6)$$

where,

K_I = Sress intensity factor for opening crack propagation mechanism (Type I).

K_{II} = Stress intensity factor for sliding crack propagation mechanism (Type II).

r = Radial co-ordinate from the crack tip

$$k = \begin{cases} 3 - 4\nu\,, & \text{Plane strain} \\ (3-\nu)\,/\,(1+\nu) & \text{Plane stress} \end{cases}$$

$G = E\,/\,(1+\nu)$ = Initial shear modulus for isotropic conditions (uncracked concrete)

ν = Poisson's ratio of concrete

U_B, U_D, V_B, V_D = Nodal displacements in the U and V directions obtained from the finite element analysis

From the stresses and strains obtained from the finite element solution at cracks in the initial state of cracking, it is possible to evaluated the orientation of principal stresses and strains that initiated the cracking and then to define the n-t axes respect to the normal and tangential direction to the crack in order to evaluate the normal and shear stresses σ_n and τ_{nt} respectively in the crack plane.

(3) Cracking stages of concrete in Finite Element Analysis

The concrete is treated as isotropic material before cracking. After cracking the concrete becomes orthotropic. The *fixed crack approach* for plane stress conditions used herein leads to an anisotropic-based stress-strain relationship for the "equivalent" continuum along the orthogonal *n-t* axes of orthotropy normal and tangential to the critical crack direction, then, initial cracking is expressed as :

$$\begin{bmatrix} \sigma_n \\ \sigma_t \\ \tau_{nt} \end{bmatrix} = \begin{bmatrix} E_n & \nu & 0 \\ \nu & E_t & 0 \\ 0 & 0 & \beta_s\,G \end{bmatrix} \begin{bmatrix} \varepsilon_n \\ \varepsilon_t \\ \gamma_{nt} \end{bmatrix} \qquad (7)$$

where,

- $\varepsilon_s = -\,(\sigma_n + \sigma_t)\nu\,/\,E_t$
- $\sigma_n = -\,\sigma_t$ and, $\varepsilon_n = -\,\varepsilon_t$ are the stresses and strains for the n-t axes.

β_s = Shear retention factor (it permits to quantify approximately the decrease of shear transfer across an existing crack). β_s is assumed to be unity if the crack is closed, and 0.5 if the crack opens. For large crack widths, the value of b_s tends to zero.

The parameter β_s takes into account the following:

a) The interlock between opposite faces of a crack when subjected to parallel differential movement.
b) The capability of shear transfer that concrete can still carry after cracking is initiated, and,
c) The *dowel effect* by means of the constrained force produced when reinforcing bars bridge the concrete cracks.

(4) Post-cracking stage

The post-cracking stage is defined as the state in which cracks are growing-up. In this stage the state of tension-shear stress is governed by the *yield condition* given by Eq. 8. This yield condition generally represents one or a combination of stress invariants and can be smooth continuous function (Von Mises) or discontinuous piece-wise linear (Tresca).

$$\sigma_n^2 + \tau_{nt}^2\,/\,\alpha^2 - f_t^2 = 0 \qquad (8)$$

The yield condition given by Eq. 10 was used by William, K., Pramono, E., and Sture, S. -1987 (Ref. 8), in order to develop the strain-softening plasticity matrix given by Eq. 9 which in turn was incorporated in the analysis discussed herein.

$$\begin{bmatrix} \sigma_n \\ \sigma_t \\ \tau_{nt} \end{bmatrix} = \begin{bmatrix} E_{11}\,(1 - 4\,E_{11}\,c\,\sigma_n^2) & 0 & -4\,c\,E_{11}\,G\,\sigma_n\tau_{nt}\,/\,\alpha^2 \\ & E_{11} & 0 \\ \text{Symm.} & & G(1 - 4\,c\,G\tau_{nt}^2\,/\,\alpha^4) \end{bmatrix} \begin{bmatrix} \varepsilon_n \\ \varepsilon_t \\ \gamma_{nt} \end{bmatrix} \qquad \ldots\ (9)$$

where,

$c = 1\,/\,(4 f'_t\,\sigma_n\,h\,E_n + 4\,\sigma_n^2 E_n + 4\,\tau_{nt}^2\,G/\alpha^4)$

$E_{11} = E/(1-\nu)^2$

f'_t = Tensile stress of concrete (See Eq. 1), (MPa)

α = Parameter from the plastic condition (See Eq. 8)

As is pointed out in Ref. 8, the dependence of the yield

$$f_{cc} = f'_{cc} \exp [-B (\varepsilon_{cc} - \varepsilon_{occ})^C] \quad (3)$$

where,

$B = (260 + 100 / f'_c) \exp (-30 f_{tr} / f'_c)$
$C = 1.2 - 0.006 f'_c$
$E_c = 3320 (f'_c)^{1/2} + 6900$ (Mpa)
$f'_{cc} = f'_c + 4.2 f_{tr}$
$\varepsilon_{occ} = 7 \times 10^{-4} (f'_c)^{1/3} + 0.06 f_{tr} / f'_c$

f_{tr} = Equivalent lateral pressure applied by the lateral reinforcement on concrete core that produces the same effect as uniformly applied pressure (MPa)

4. Bond stress of steel reinforcing bars in a reinforced concrete member under tension effects

The RC piers that were subjected to the strong shaking of the 1995 Great Hanshin Earthquake had been undoubtedly subjected to relatively high levels of axial loads (in both tension and compression) produced by the large bending moments dynamically generated, especially in the lower part of piers at which plastic hinges may produce. It implies that, concrete was most likely to be in tension and cracked, so, the bond stress produced by both the horizontal component of the bearing forces exerted by the lugs and the vertical component of the bearing force which creates a radial force responsible for splitting the surrounding concrete, were significant. On this way, it is necessary to consider properly the effect of bond stresses in the analysis of RC piers subjected to strong ground motions.

Finite element analysis could be used for bond behaviour to calculate the concrete-to-steel reactions, but, the validation of such results will depend strongly on the features considered in both the mathematical model and analysis process including the high sensitivity of the mesh under cyclic reversals. Herein, the bond stress of steel reinforcing bars is considered by partially using Eq. 4 (See Fig. 4), which was proposed by the 1990 CEB-FIP Model Code[5] on basis of an average of available relationships obtained from pull out tests.

$$\tau_b = \tau_{max} (s / s_1)^{\eta} \quad (4)$$

where,

τ_{max} = bond strength,
s = slip,
$0 \le \eta < 1$, η is an experimental constant

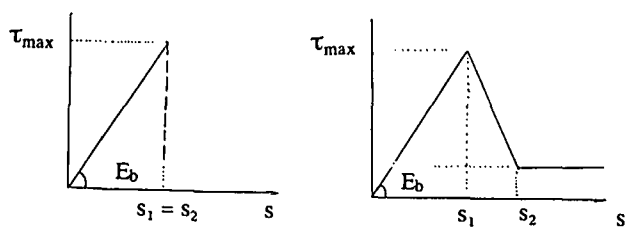

a) initial stage b) subsequent stages

Fig. 4 Adopted bond stress-slip curves

a) For deformed bars in confined concrete

In this case, the concrete fail by shearing off between ribs. It requires that :

$$c \ge 5 d_b ,$$

- c = Thickness of concrete cover (measured from the tension face to the surface of tensioned bars.
- Bar spacing > 10 d_b or closely spaced stirrups
- $\tau_{max} = 2.5 f'_c$ (MPa) , $s_1 = 1.0$ mm , $\eta = 0.4$

b) For deformed bars with no or little amount of transverse reinforcement

In this case, the failure is given by splitting of the concrete cover. It is supposed to occur when :

- $c = d_b$
- $\tau_{max} = 2.0 f'_c$ (MPa) , $s_1 = 0.6$ mm , $\eta = 0.4$

Note : The parametric values s_1 and η are valid for bars with a relative rib area close to 0.08.

5. Nonlinear finite element analysis of concrete cracking by using the smeared - crack approach

The smeared crack approach (orthogonal fixed crack model) is used herein for numerical modeling of crack initiation and crack propagation. Under this model, the crack orientations are assumed to not change during the remaining part of the analysis. The calculation of the crack width "h" is based on the failure states corresponding to *Mode I* (tearing) and *Mode II* (in-plane shear) failure types of linear fracture mechanics theory applied to concrete structures.

At this point, it is important to remark that the applicability of conventional concepts to concrete is not easy, due to the heterogenity of concrete (a composite, multiphase material).

Cracks are initiated when stresses exceed the strength of the material and propagate according to fracture mechanics if the release energy during crack propagation is larger than the fracture energy needed to propagate the crack. On this way, the Bazant's relationship[6] (Eq. 7) to predict the softening modulus of concrete (E_t) in function of the fracture energy (based on a linear tensile-stress-strain softening diagram) can be considered if the crack band width h and the fracture energy G_f are known. This makes possible to transform the discrete crack behaviour into the smeared crack approach.

$$E_t = f'^2_t \, h / 2G_f \quad \text{(MPa)} \quad (5)$$

where ,

E_t = Softening modulus of concrete (Mpa)
f_t = Tensile stress of concrete (See Eq. 1), (MPa)
G_f = Fracture energy (MPa)
h = Crack band width, assumed to be approximately three times the maximum aggregate size of the concrete

(1) Idealization of crack tip

The boundary comformity of displacements around the crack tip obtained from the finite elemet analysis can be enforced by using displacement correlation[7] with the quarter-point element in order to remove the non-convergence conditions caused around the crack tip. It is a

condition (See Eq. 9) on the shear stress τ_{nt} introduces the term between the principal normal stresses and shear strains due to stress-induced anisotropy as well as the term that takes into account the shear stiffness.

6. Numerical computation

Due to the nonlinearity introduced in the computational model through the stress-strain relationship of concrete, the dynamic equilibrium equation is solved in the time domain, following a step-by-step procedure.

A predictor-corrector Newton-Raphson scheme is used to linearize the equations for each time step of the time integration process. Bond is considered by the introduction of bars geometry. Concrete strains at cracking or yielding are obtained by comparing the strain in the concrete computed from the analysis with the limiting strains defined by the stress-strain relationships for both tension and compression (See Eqs. 1 through 3). Similar procedure is applied for the evaluation of cracking and yielding stresses.

7. Model problem and input motion

(1) Model problem

The model analized herein, consists of a reinforced concrete single-bent pier supporting a typical steel girder as shown in Fig.6. Supporting atop of the piers is given by fixed bearing supports. The soil conditions are not taken into account in the analysis.

The pier model was selected on basis of the type of bridge piers that sustained severe damage or collapsed during the 1995 Great Hanshin Earthquake. Nominal concrete properties such as the mass density, the Young's modulus, the Poisson's ratio and the fracture energy are taken to be 2500 kg/m^3, 30000 MPa, 0.2 and 200 N/m, respectively. The compressive strength is assumed to be f'_c = 40.0 MPa while the damping was set to 5.0 percent of the critical value. The modulus of elasticity E_S for the steel reinforcing bars was assumed to be 199,955 MPa (2.9x10^7 psi). The mesh considered is shown in Fig. 7. The elements are triangular without to be necessary symmetrics.

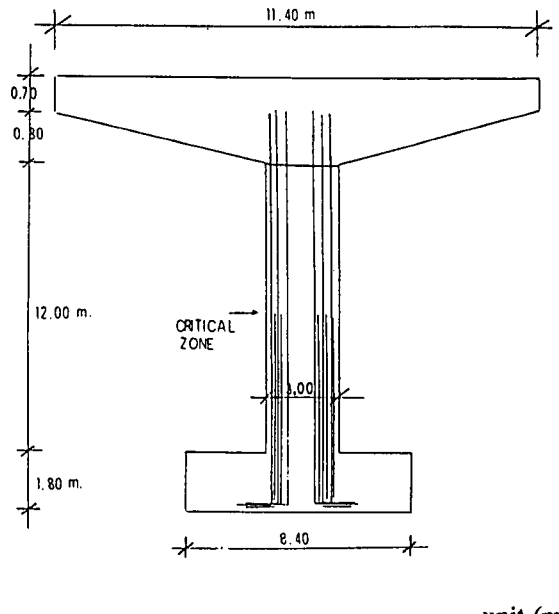

Fig. 6. Geometric characteristics of the bridge pier

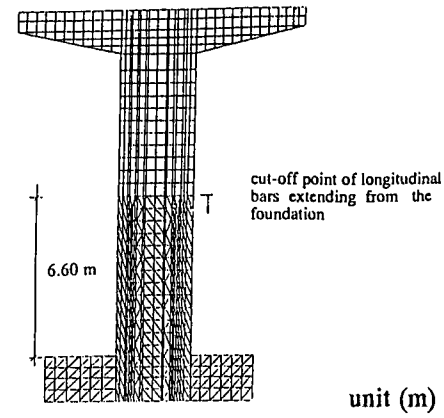

Fig. 8. Finite element mesh for the model problem

The analysis is performed using a uniform piece-linear wave of 4 seconds of duration with peak acceleration of 0.4 G (See Fig. 7). The time step considered was 0.01 sec.

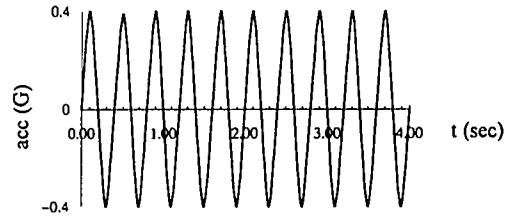

Fig. 7. Input motion considered in the analysis.

8. Numerical results

In the following, analytical results on the dynamic behaviour of the RC single-bent column aboved described are presented. These results are compared with the behaviour of RC single-column bents that sustained heavy damage or collapsed during the 1995 Great Hanshin Earthquake.

At first, the variation of cracking moments (moment produced in a cross-section of the pier after reach its cracking stage) along the height of the pier, from the base to the top, is plotted in Fig. 9. From this figure it is possible to infer that global response of the pier in the zone ranged from the top to approximately the cut-off line of bars extending from the base (See Fig. 6), diverges only slightly from linear. Below this cut-off line the curve shows also a slightly nonlinearity, it may indicate that the bent started to develop flexural cracks (cracks at approximately right angles to the longitudinal axis of the pier) which started to propagate downward.

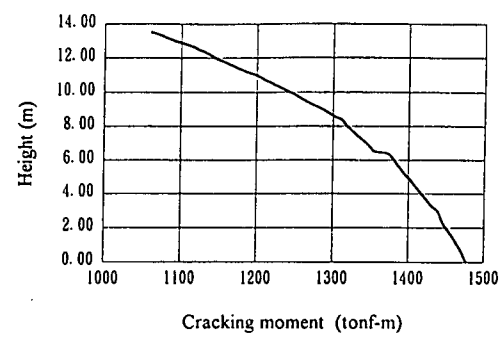

Fig. 9. Variation of cracking moments along the height of the pier

In order to evaluate the probably mechanism in the concrete core, it is of much importance to know the rotations produced in a cross section when cracking occurred.
Fig. 10 depicts the variation of rotations in the cracking stage by means of the rotation angles produced after cracking had occurred at several locations along the height of the pier. This plot indicates effectively an approximate linear elastic response with the exception of the rotation produced at the cut-off line of longitudinal bars extending from the foundation. From this figure, it is noticed that the variation of rotaions are defined by two parts, the upper part seems to demostrate that cracking has started to propagate slightly and uniformly upward and with several patterns downward such as flexural cracks and inclined cracks. Nonetheless, the small rotations upward in the zone above the cut-off line seems to indicate that cracks propagating upward remain relatively narrow.

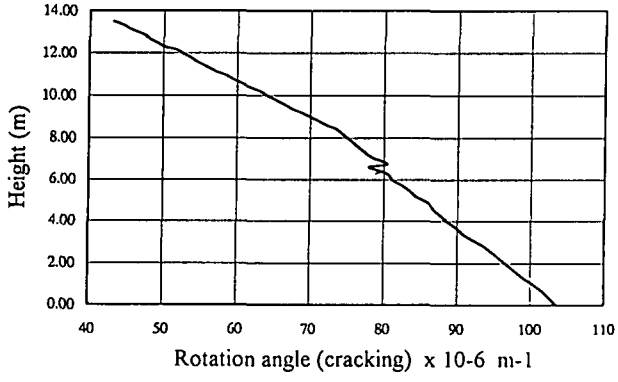

Fig. 10. Rotation angles produced in cracking stage versus height of the pier

Fig. 11 presents the concrete strains when cracking has reached at several locations along the height of the pier. This figure demonstrated that cracking of concrete started to form at relative low strains with a maximum value of approximately 0.00058 at the base of the pier.
The variation of both rotations and strains at the cracking stage showed by Figs. 10 and 11, indicates that spalling is the first mechanism to have occurred, spalling of concrete seems to start to develop from about the cut-off line in both directions downward and upward.

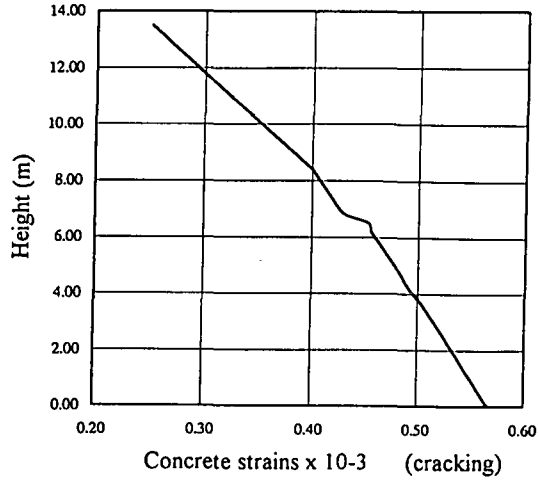

Fig. 11. Variation of the concrete strains in the cracking stage along the height of the pier

Rotations produced as consequence of yielding are plotted in Fig. 12 for several sections along the height of the pier. From this figure, it is possible to state that the RC single-column bent exhibit the largest amount of apparent yielding just immediately above the cut-off line, it is because of the reduction of the effective area of steel reinforcement. Although is not shown in this figure, strains in the upper part of the pier remained below the nominal yield value. However, some strains, especially around the cut-off line, exceeded the yield value.

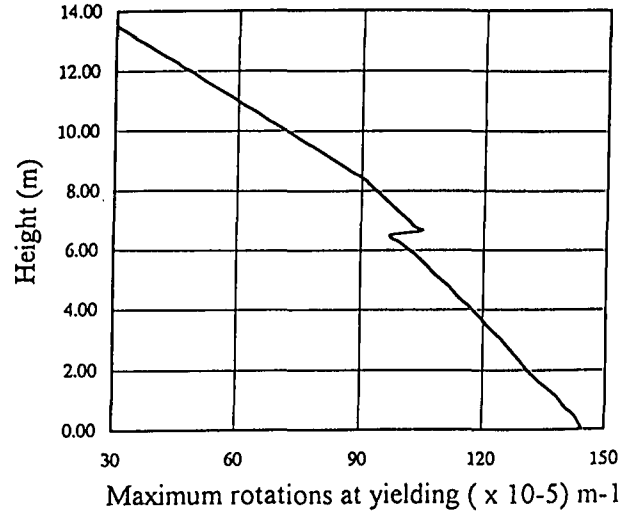

Fig. 12. Maximum rotations along the height of the pier after yielding has reached

Finally, the maximum displacements at yielding is plotted in Fig. 13 along the height of the pier. A maximum yield displacement of about 6 cm is produced at the top of the pier after yielding in the cut-off line is produced.
The displacements exhibit small values relatively, it may be due to the uniformity of the input motion (piece linear wave) applied as well as the relatively moderate value for the maximum acceleration (0.4 G).

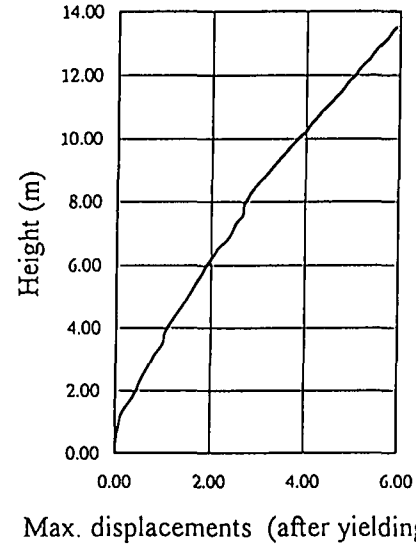

Fig. 13. Maximum displacements along the height of the pier after yielding has reached

9. Final considerations

It can be regarded that *reversing plastic hinges*. are formed as consequence of the inelastic deformation cycles during a strong shaking. With a change in the direction of sway, the direction of inelastic rotation sustained by each of the plastic zones reverses. This results in the formation of cracks and then the initiation of the failure mechanism.

By this way, a change in the direction of a rotation near the base of the pier will imply the starting of a bending failure mechanism while if this change in the direction of rotation occurs in the vicinity of the midheight of the pier, it will imply the formation of shear failure mechanism or flexural-shear mechanism (See Fig. 14).

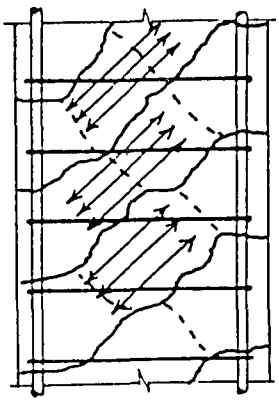

Fig. 14. Shear mechanism in a plastic hinge zone

During the process of failure, such inelastic rotations accumulate in the pier at plastic hinge zones. On the other way, the maximum lateral displacement of the upper deck can be estimated by taking into account the maximum rotation of the plastic hinge located in the lower part of the pier by using the simplified model of a single-column bent proposed by Priestley and Park (1987), described by Eq. 12 and depicted in Fig. 15.

$$d_{max} = d_t + d_f + d_y + d_p \qquad (12)$$

where,

d_t and d_f = Translation and rotation contributions of the foundation

d_y = deformation of the pier when yielding is first reached at the base

d_p = Maximum admisible rotation of the plastic hinge located in the lower part of the pier

$d_p = (f_p . L_p)\,(H - L_p/2)$

On this way the deformations of the pier at lower part of the pier when yielding is reached (d_y), as well as, the maximum admisible rotation (estimated from the maximum rotations), obtained from an analysis such as the presented herein may be considered.

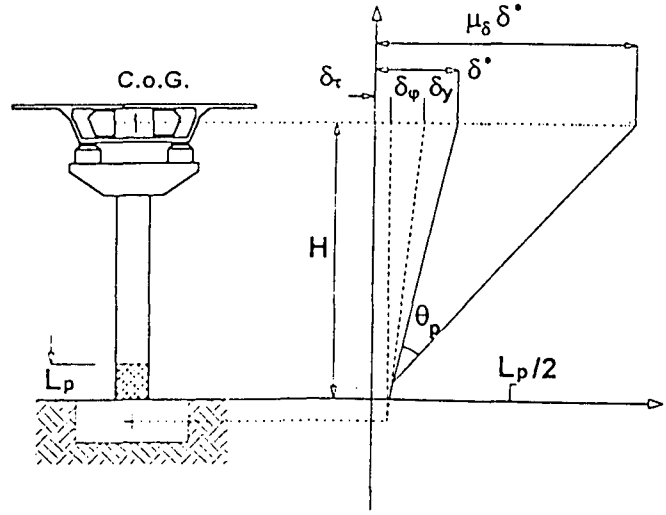

Fig. 12 Components of total displacement including the foundation effects [(after Prietley and Park (1987)][9]

10. Conclusions

Based on the results of this study, the following conclusions can be drawn.

From this study, it seems to be that the same level (at the same height) for the cut-off point of longitudinal bars extending from the foundation was a very important factor that caused to rotations to change bruscally at such point and consequently the cause of the formation of plastic hinges in the zone starting from just below the cut-off point to the base of the pier. It combined with the inadequacies in the structural detailing as well as with the poor confining reinforcement, caused failure to be of the flexural-shear type. This failure mechanism correlates well with the typical flexural-shear failure observed in a large amount of RC single-column bents supporting the Hanshin Expressway in Kobe area.

The writers felt that an accurate characterization of the mechanical behavior of development length (splices) , as well as of reinforcing steel bars extending from the foundation under cyclic reversals is needed in order to establish a firm basis in the quantification of bond strength. In view of this, laboratory tests may help to define more clearly such characterization which must accurately account for the effects of concrete cover, bar spacing, and confining reinforcement, since these parameters play a critical role in bond strength.

References

1. Takada, S., Morikawa, H., and Duran, F. " Survey on Seismic damage to Bridges on Highways and Railways caused by the 1995 Great Hanshin Earthquake", Kobe University, special publication, March 1995.

2. Kim, J. K., and Lee T. K., " Failure Behaviour of Reinforced Concrete Frames by the Combined Layered and Nonlayered Method," *Comput. Struct. J.* 1993, 48(5), pp. 819-825.

3. Otter, D . E., and Naaman, A. E., " Model for Response of Concrete to Random Compressive Loads, " *J. Struct. Engng*, ASCE 1989, **115**(11), 2794-2809.

4. Saatcioglu, M., and Razvi, S. R., " Strength and Ductility of Confined Concrete," *J. of Struct. Engng*, ASCE, V.118, N. 6, 1988, pp. 1590-1607.

5. CEB BI 124 /125 , " Model Code For Concrete Structures," April 1978.

6. Bazant Z. P.," Mechanics of Distributed Cracking," *Appl. Mech. Rev.*, ASME, 39 - 5) , pp. 675-705, 1986.

7. Shih, C . F., De Lorenzi, German, M. D., " Crack Extension Modeling With Singular Quadratic Isoparametric Elements,"*Int. Journal Fract..*, Vol 12, pp.647-651, 1976.

8. William, K., Pramono, E., and Sture , S. " Fundamental Issues of Smeared Crack Models, " SEM/ *RILEM ,"* International Conference on Fracture of Concrete and Rock, Houston, Texas, June 1987, Editors: S.P.Shah,

9. Priestley, M. J. N., and Park, R., " Strength and Ductility of Concrete Bridge Columns Under Seismic Loading," ACI Struct. J., 84(1). pp. 61-76, 1987.

阪神大震災によるＲＣ橋脚の破壊メカニズムに関連するひび割れ挙動

神戸大学　高田至郎
神戸大学　森川英典
神戸大学　Freddy Duran C.

本研究は、異方性離散ひび割れモデルを考慮した非線形有限要素法を用いてＲＣ橋脚の地震時応答におけるひび割れ挙動を解析することを目的としている。鉄筋との付着を考慮したコンクリートの劣化とひび割れ破壊を考慮するため、コンクリートのひずみ軟化が考慮される。また、鉄筋とコンクリートの付着破壊モデルも考慮される。本研究における解析は、阪神大震災で大被害を受けた典型的なＲＣ橋脚と類似のモデルに対して行われる。解析結果から、ＲＣ橋脚の地震時応答におけるひび割れ挙動の解明に寄与する考察と提言が示される。